Comparison of Boost Chopper and Active Buffer as Single to Three Phase Converter

Yoshiya Ohnuma
Student Member, IEEE
Nagaoka University of Technology
1603-1 Kamitomioka-machi Nagaoka City
Niigata, Japan
ohnuma@stn.nagaokaut.ac.jp

Jun-ichi Itoh
Member, IEEE
Nagaoka University of Technology
1603-1 Kamitomioka-machi Nagaoka City
Niigata, Japan
itoh@vos.nagaokaut.ac.jp

Abstract—**This paper presents a comparison in terms of efficiency and volume between the single-to-three-phase power factor correction (PFC) converter. A conventional PFC circuit that consists of a boost chopper requires a large boost-up inductor and large smoothing capacitors to decouple the power ripple. The size and efficiency of the converter become a discussion issue recently. On the other hand, a single-to-three-phase power converter using an active buffer has been proposed. The active buffer does not require a large inductor and large smoothing capacitors in the DC link part. These two types of converters are designed and simulated to calculate the losses. In addition, a prototype converter has been built and tested. The efficiency achieves 94.6% at 1.5-kW same as the calculated efficiency. Furthermore, the efficiency increases by 1.5% comparing to the conventional converter. In addition, the volume is decreased by approximately 0.7 times then the size of the conventional converter.**

I. INTRODUCTION

Single-phase to three-phase converters achieve energy saving in the application of home motor appliances. One of the important requirements of the converter is to provide low input current harmonics. Therefore many power factor correction (PFC) converters and control methods have been proposed [1]-[3]. At the same time, studies on the high efficiency and design of the volume are very important subjects in this field. The most common structure of PFC converter is the single-switch boost chopper circuit (conventional converter) as shown in Fig. 1 [1]. This circuit can control the input current easily. However, this converter requires a large boost-up inductor and a large smoothing capacitor to decouple the power ripple, which is a frequency twice of the power supply at the DC link part. In addition, the DC link voltage is always higher than the maximum input voltage because a boost-up converter is used. Therefore the switching loss of this conventional converter becomes high.

In order to reduce the volume of the smoothing capacitor, some power decoupling converters have been proposed [4],

[5]. These circuits add the a few switching devises and energy buffer such as capacitor or reactor to the conventional boost chopper. Certainly, the voltage ripple in the DC part can be reduced by the control of the energy buffer even if the small something capacitor is used in DC part. However, the additional circuit for the power decupling causes increasing the power loss.

Apparently, a single-to-three-phase power converter with an active buffer (proposed converter) as shown in Fig. 2 has been proposed in [6] in terms of loss reduction of the power decoupling circuit. This converter is based on the concept of an indirect matrix converter that coupled with an active buffer to decouple the power ripple. The converter obtains sinusoidal waveforms on the input and output current. In addition, the size of the converter is reduced because the converter does not require a large smoothing capacitor and a large boost inductor in the DC link part. However, the clarifying of the efficiency and the volume are remained unidentified.

This paper demonstrates a comparison on the efficiency and the volume among these converters. At first, the paper discusses the circuit layout and control methods for these single-to-three-phase PFC converters. There are two type of boost up operation modes which are known as the continuous current mode (CCM) and the discontinuous current mode (DCM). Second, each parameter of the passive components is designed and utilized in the simulation analysis in order to compare the losses of these converters.
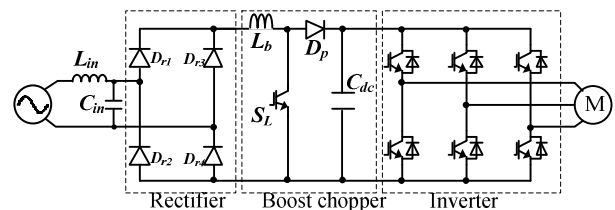

Fig.1 Conventional converter.

515

Then the size of the heat sink is calculated based on the simulation results. Nevertheless, a prototype of the proposed converter has been built and tested in order to validate the loss analysis. As a result, the efficiency of the proposed converter is 1.5 % higher than the conventional converter with DCM boost chopper. In addition, the total volume of the passive components is approximately decreased by 0.7 times comparing to the conventional converter with CCM boost chopper.

II. CIRCUIT CHARACTERISTICS

Figure 1 shows a single-to-three-phase converter with a single switch boost converter. The converter consists of a diode rectifier, inverter and boost chopper. There are many control methods can be applied into this PFC [1]-[3]. The point of the control method is as following.

- The current of an inductor is either CCM or DCM.

- Duty ratio of the switch in boost chopper is either constant or variable.

- Frequency of the switch in boost chopper is either constant or variable.

The simplest controls such as constant duty ratio, constant frequency or line frequency commutated control can obtain high power factor easily for low power applications. However, the input current remains distorted at low voltage boost ratio. On the other hand, advanced control strategies can control the input current into a clear sinusoidal waveform based on the duty ratio or switching frequency. In this paper, CCM or DCM operation with constant switching frequency and variable duty ratio methods are discussed.

Figure 2 shows a single-to-three-phase converter with an active buffer [6]. The active buffer that consists of a discharge circuit and a charge circuit replaces the boost chopper to decouple the power ripple, which the power ripple has a frequency that is twice of the power supply. The discharge circuit consists of a small capacitor and a switch. The charge circuit is similarly to a boost chopper circuit but using a smaller inductance value because the current is controlled based on DCM. The voltage ripple in the DC link part is absorbed to the small capacitor C_{dc} by controlling its terminal voltage. The terminal voltage of C_{dc} has large fluctuation according to the energy ripple which comes from the input side.

Figure 3 shows three different control method diagrams for PFC circuits. The switching duty ratio d_l of CCM is obtained by PI controller using the inductor current as shown figure 3 (a). In contrast, DCM can obtain the duty d_l using the equation without a current sensor as follows:

$$d_l = \sqrt{\frac{2L_b(v_c - v_{in})i_l^*}{v_{in}v_cT_{sw}}} , \qquad (1)$$

where, L_b, v_c, v_{in}, i_l^* and T_{sw} are inductance of the boost-up inductor, DC link capacitor voltage, input voltage, inductor
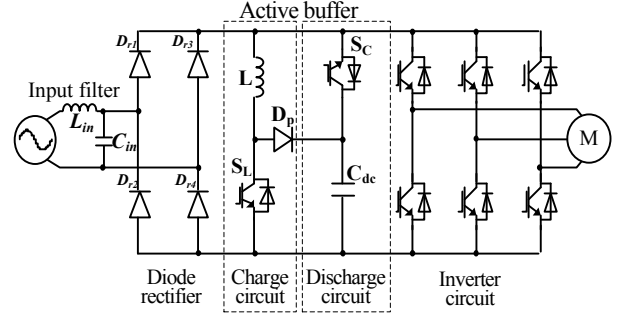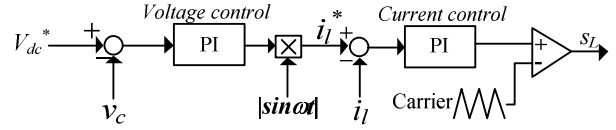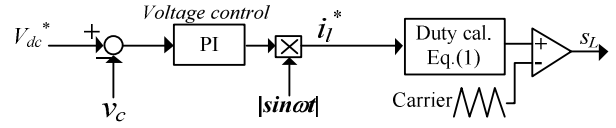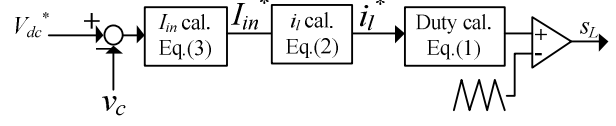

Fig.2 Proposed converter.

(a) Conventional converter with CCM

(b) Conventional converter with DCM

(c) Proposed method

Fig.3 three different control method diagrams for PFC circuits.

current command and switching period of the switch in boost chopper, respectively.

Therefore, for both the conventional converters, the inductor current command i_l^* is obtained by a PI controller.

In the proposed control method, the power ripple is compensated by the discharge circuit and the charge circuit. The control method of the charge circuit is based on the DCM. Therefore the duty ratio is determined by (1). It should be note that the charge circuit and the discharge circuit are operating alternately at per quarter cycle of the power grid frequency. Thus, half of the input power is supplied directly to the inverter. Therefore the inductor current command i_l^* is calculated by

$$i_l^* = I_{IN}|\sin(\omega t)| - \frac{I_{IN}^*}{2|\sin(\omega t)|} , \qquad (2)$$

where I_{IN}^* is the amplitude of the input current command and ω is the input single phase angular frequency In addition, the capacitor voltage is fluctuating in this system. Hence, the power ripple W_C which is the electric storage energy is calculated by the maximum capacitor voltage V_{Cmax} and

minimum capacitor voltage V_{Cmin}. Therefore $I_{IN}{}^{*}$ can be expressed by

$$I_{IN}{}^{*} = \frac{2\omega W_C}{V_{IN}} = \frac{\omega C_{dc}}{V_{IN}}\left(V_{C\max}{}^2 - V_{C\min}{}^2\right), \qquad (3)$$

where V_{IN} is the peak value of the input voltage, C_{dc} is capacitance of the DC link capacitor. Notice that the proposed circuit is not implemented with the PI controller, as a result, the transient response for the control of DC link voltage is fast and stable.

III. DESIGN OF PARAMETERS

This section explains a design example for a 1.5- kW class PFC converter. Table 1 provides the common specification of the converters.

A. Input filter

The input filter for PFC circuit must have enough ripple attenuation at per switching frequency to satisfy the EMI requirement. In order to satisfy the above requirements, the cut-off frequency is required to be lesser than 1/5 to 1/10 times of the switching frequency. In this case, we design the cut-off frequency f_{cf} sets to 1.5 kHz. Also, in order to control the input power factor closed to unity at the line frequency, the reactance of input filter L_{in} is set to 1 % of rated impedance of converter. From these specifications, we obtain

$$L_{in} = \frac{\% L Z_{\text{cov}}}{2\pi f_{in}} = \frac{0.01\dfrac{200}{7.5}}{2\cdot\pi\cdot 50} = 0.85\ mH\ , \qquad (4)$$

$$C_{in} = \frac{1}{L_{in}\left(2\pi f_{cf}\right)^2} = \frac{1}{0.85\cdot 10^{-3}\left(2\pi 10\cdot 10^3\right)^2} = 13.2\ \mu F \qquad (5)$$

B. Boost-up inductor L_b

This section discusses the design of the boost-up inductor. In order to simplify the derivation, we design the inductor value based on the peak value of the input voltage. At the input phase of $\pi/2$, the peak value input voltage is V_{IN} and the capacitor voltage is assumed as the average value V_C.

First of all, the ripple of the inductor current is discussed. The inductor current ripple ΔI_L is obtained from

$$\Delta I_L = \frac{V_L}{L_b}\Delta t_{on}\ , \qquad (6)$$

where Δt_{on} is turn on time of the switch in the boost chopper and V_L is inductor voltage of the boost-up inductor. V_L equals v_{in} when the switch is turned on. In contrast, when the switch is turned off, V_L equals to v_c minus v_{in}. Therefore, we obtain Eq. (7) at the maximum ripple of the inductor current.

$$0 = \frac{V_{IN}}{L_b}\Delta t_{on} - \frac{V_C - V_{IN}}{L_b}\left(T_{sw} - \Delta t_{on}\right)$$

$$\Delta t_{on} = \frac{V_C - V_{IN}}{V_C}T_{sw} \qquad (7)$$

Table 1 Common specification of converters.

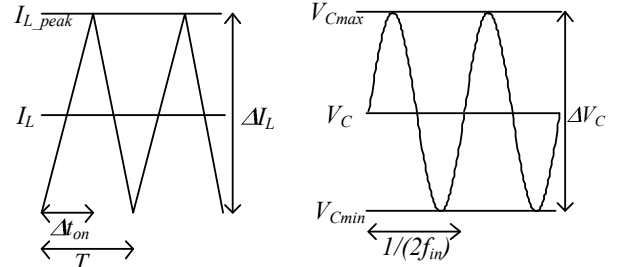| Items	Value	Items	Value
Input voltage (rms)	200 V	Average capacitor voltage	350 V
Input frequency	50 Hz	Carrier frequency	10 kHz
Input filter L_{in}	0.85 mH	Output power	1.5 kW
(% impedance)	1 %	Output frequency	50 Hz
Input filter C_{in}	13.2 μF	Tempera ture	Ambient	40 °C
(% impedance)	0.02 %		Junction	125 °C

Fig.4 Definition of inductor current and capacitor voltage parameters.

From Eq. (6) and (7), the required inductance of the boost-up inductor L_b is obtained by

$$L_b = \frac{V_{IN}(V_C - V_{IN})}{2V_C I_L \Delta I_L f_{sw}}\ , \qquad (8)$$

where f_{sw} is the switching frequency of the chopper.

Here, the current ripple ratio r_l of the inductor, which is normalized by the peak value I_L of average inductor current for one switching period is expressed in Eq.(9).

$$r_l = \frac{\Delta I_L/2}{I_L}\ . \qquad (9)$$

Therefore Eq. (8) can be rewritten as

$$L_b = \frac{V_{IN}(V_C - V_{IN})}{2V_C I_L r_l f_{sw}}\ . \qquad (10)$$

The required inductance of the boost-up inductor L_b is dominant at the maximum inductance current I_L and the ratio of the inductor current ripple r_l. Note that in the inductor current, the ratio of the inductor current ripple r_l is from 0 to 1 means that the inductor current is a continuous current (CCM). Over than 1 means the inductor current is controlled as a discontinuous current (DCM). Then the peak values of the each current mode are calculated by

$$\begin{aligned} I_{L\_peak} &= I_L r_l + I_L\quad,\text{when}\quad r_l < 1\,(\text{CCM})\\ I_{L\_peak} &= 2I_L r_l\quad,\text{when}\quad r_l \geq 1\,(\text{DCM}) \end{aligned} \qquad (11)$$

From (11), I_{L_peak} of DCM becomes twice of the I_L and more.

In term of design, we assumed that the ripple ratio of inductor current r_l for CCM is lower than 0.1 p.u. For the comparisons, r_l parameter for the DCM and proposed converter needs to be 1.1 p.u. From the calculation, the boost-up inductor L_b is obtained as shown in Table 2. Notice that in the proposed circuit, the value of inductor current I_L is half of the conventional converters as shown in Eq. (2).

C. DC capacitor C_{dc}

In the single-phase to three-phase converter, the electric storage energy required to compensate the power ripple W_C is obtained by

$$W_C = \frac{1}{2} V_{IN} I_{IN} \int_0^{\frac{1}{4f_{in}}} \sin(2\omega t) dt$$
$$= \frac{V_{IN} I_{IN}}{2\omega_{in}} \qquad (12)$$

where I_{IN} is the amplitude of the input current and ω_{in} is the input single phase angular frequency. Moreover, the W_C in the capacitor is required from the relations between the electric power and the capacitor voltage by (13).

$$W_C = \frac{1}{2} C V_{C\max}^2 - \frac{1}{2} C V_{C\min}^2, \qquad (13)$$

where, V_{Cmax} is the maximum voltage, and V_{Cmin} is the minimum voltage of the buffer capacitor.

The electric storage energy used to compensate the power ripple W_C is obtained by (12) and (13). Therefore, the minimum capacitance in the buffer circuit is obtained by (14).

$$C_{dc} = \frac{2W_C}{V_{C\max}^2 - V_{C\min}^2}$$
$$= \frac{V_{IN} I_{IN}}{\omega(V_{C\max}^2 - V_{C\min}^2)} \qquad (14)$$

The capacitance C_{dc} is obtained from the ratio of the capacitor voltage ripple r_c which is expressed in (15). The capacitor voltage ripple r_c is normalized by the average value V_c of the capacitor voltage for a grid period.

$$r_c = \frac{\Delta V_C / 2}{V_C} \qquad (15)$$

Accordingly, the capacitance C_{dc} is obtained from

$$C_{dc} = \frac{W_C}{\omega_{in} V_C^2 r_c}$$
$$= \frac{V_{IN} I_{IN}}{4\omega_{in} V_C^2 r_c}, \qquad (16)$$

Therefore the capacitance C_{dc} depends on the peak-peak voltage ΔV_C.

In the conventional converters, the DC capacitor voltage must be sufficiently higher than the maximum input voltage to control the PI controller stable. Therefore, we assume the ratio of the capacitor voltage ripple r_c parameter is 2.5%. In

Table 2 Design value of parameters

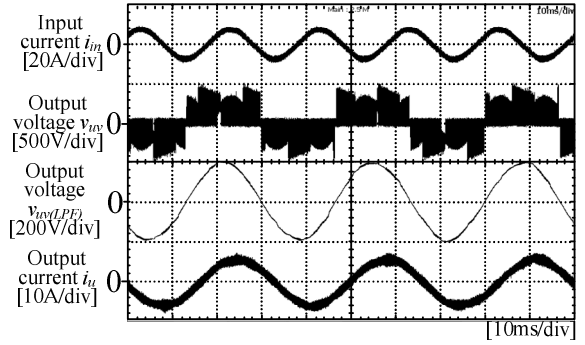| Items		Proposed converter	Conventional converter (CCM)	Conventional converter (DCM)
Boost Inductor	r_l	1.1 p.u.	0.1 p.u.	1.1 p.u.
	L_b	0.46 mH	2.6 mH	0.23 mH
	I_L	5.3 A	10.6 A	10.6 A
	I_{L_peak}	11.7 A	11.7 A	23.3 A
DC-link capacitor	r_c	0.143 p.u.	0.025 p.u.	0.025 p.u.
	ΔV_C	100 V	17.5 V	17.5 V
	C_{dc}	Required : 136 uF Selected : 150 uF	Required : 136 uF Selected : 150 uF	Required : 136 uF Selected : 150 uF
	Rated ripple current	5A	5A	5A

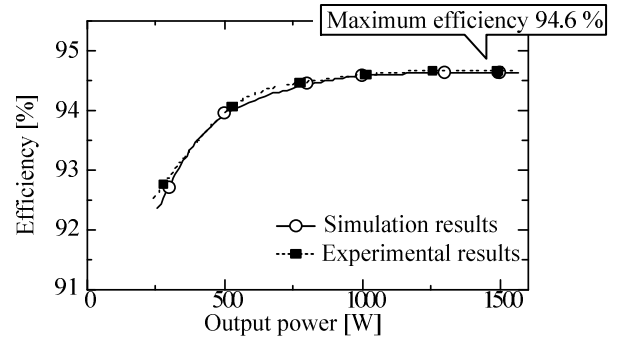Fig. 5 Experimental results of proposed converter.

Fig. 6 comparison efficiency between experiments and simulations.

the proposed converter, the fluctuation of the DC capacitor voltage can be controlled by the active buffer. Therefore the ratio of capacitor voltage ripple r_c parameter is set to 14.3%. So, requirements for capacitance C_{dc} of these converts are obtained as shown in Table 2. However, the selection of the electrolytic capacitor must consider upon its rated ripple current. Therefore, we select the closest capacitor that meet these conditions as shown in Table 2.

IV. COMPARISON OF LOSSES

This chapter shows the loss analysis using the circuit simulator Piece-wise Linear Electrical Circuit Simulation (PLECS). We assume that each winding resistance of the inductor is same as 0.25 Ω. The motor condition is simulated by ideal current sources. Here, the rated voltage of the motor specification is generally 200 V. However, in the proposed

converter, the voltage transfer ratio between the input voltage and the output voltage is less than 0.707 because the principle of the converter is a step-down converter. Therefore the motor rating for the proposed converter is changed to 141 V.

In order to validate the simulation results, the proposed converter has been tested practically. The experimental conditions are the same as the simulation, in Table 1 and 2. Figure 5 shows operation waveforms of the proposed converter. Sinusoidal waveforms are obtained on the single-phase input current and three-phase output current, with a single-phase power factor of over 99 %.

Figure 6 shows the comparison of the efficiency between experiments and simulations. The proposed system can achieve efficiency 94.6 % similar to the simulated loss analysis. Moreover, simulation results of the loss can achieve approximately the same efficiency to the experimental results at any range. That is, those experimental results confirmed that the power loss for each converter can be discussed based on loss simulations.

Figure 7 shows loss comparisons among the three converters. The total efficiency of the proposed converter is increased by 0.7 % comparing to the CCM. The largest difference shown in the loss is the boost inductor loss. DCM shows the largest in the boost inductor loss because the peak current is the highest among these converters. (Refer to Table 3). In the proposed converter, although the peak current is equal to CCM, the amount of current flows into the boost-up inductor is nearly quarter of the CCM.

Figure 8 shows a study on the losses among the boost choppers (conventional circuits) and the active buffer (proposed converter). The loss of the active buffer is decreased by 10 to 20 % in compared with the conventional boost choppers. In particular, even the number of switches is increased in the active buffer, but the current passing through the active buffer is quarter of the input current. Therefore the conduction loss is decreased.

V. DESIGN OF CONVERTER VOLUME

A. Inductor

The design of the inductor volume can be calculated by using an area product method [7]. The area product A_p is defined as following

$$A_p = A_e A_w , \qquad (17)$$

where A_e is the cross-sectional area of magnetic core, A_w is the cross-sectional area of the winding wire as shown Fig. 9. The area product A_p can obtain the volume due to bisect A_e and A_w at right angles. The volume of an inductor can be related to the area product A_p. The relationship is derived according to
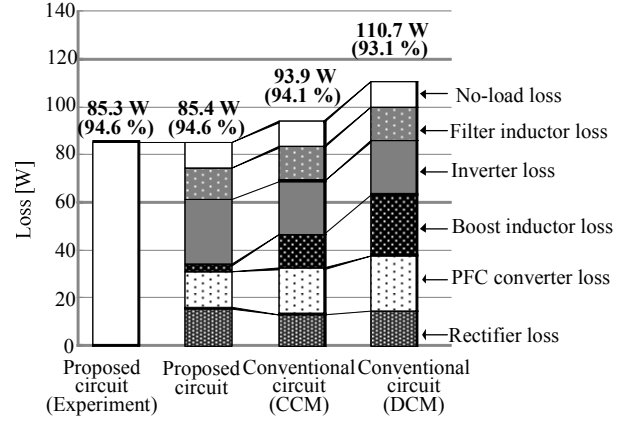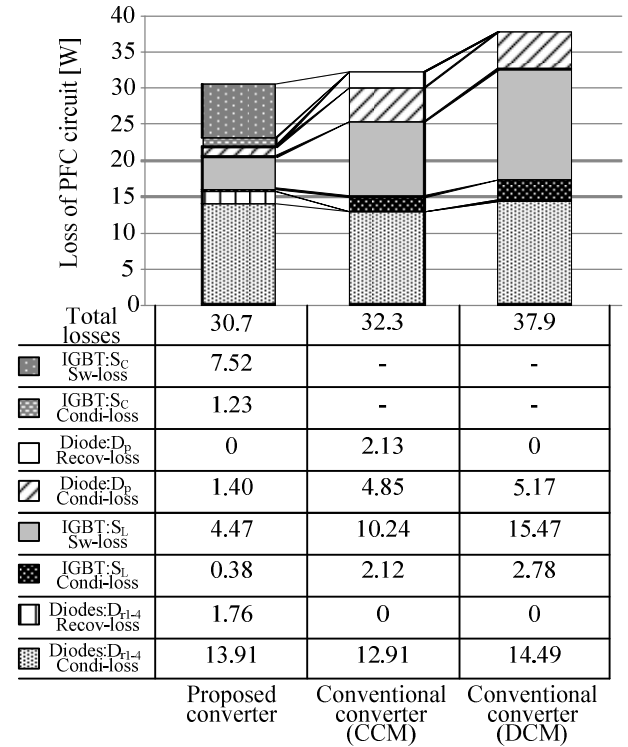

Fig.7 Loss analysis of converters.
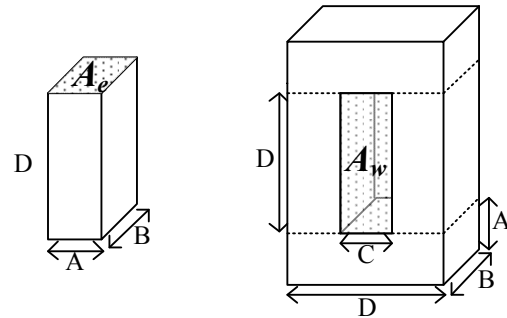

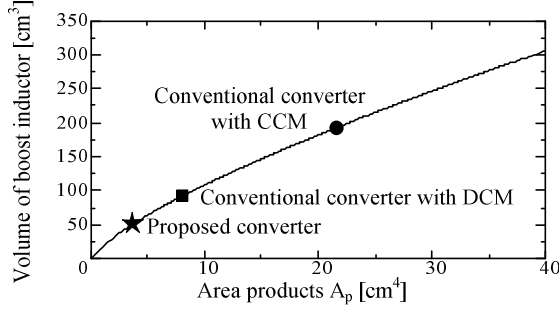Fig.8 Detail loss analysis of PFC converters.

Fig.9 Design of core.

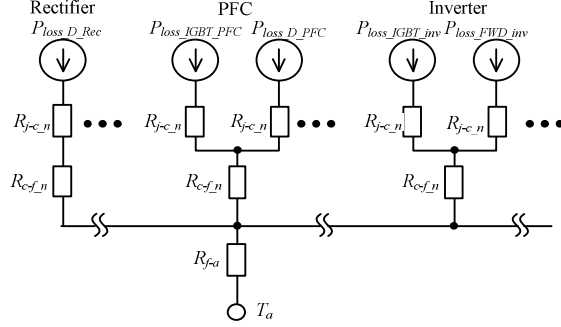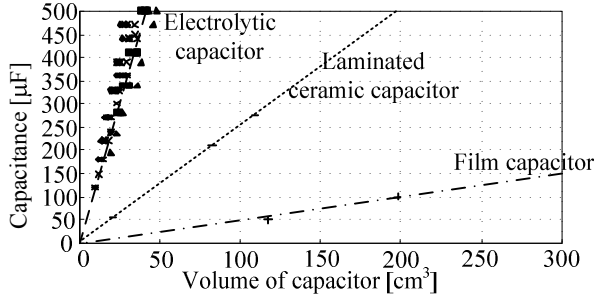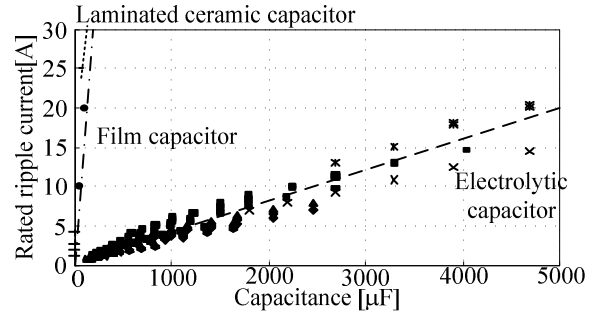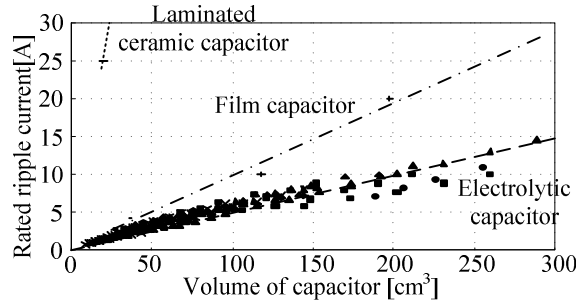Fig. 10 Relationship between the inductor volume and the area products.

Fig. 11 Simplified thermal model.

(a)Volume of capacitor versus capacitance

(b) Capacitance versus Rated ripple current

(c)Volume of capacitor versus rated ripple current

Fig. 12 Relationship among volume of capacitor, capacitance and rated ripple current.

$$V_L = K_V A_p^{\frac{3}{4}} \ , \tag{18}$$

where K_V is a constant related to core configuration values.

The area product of an inductor is obtained as

$$A_p = \frac{2W_m}{K_u B_m J_w} \ , \tag{19}$$

where W_m, K_u, B_m and J_w are the energy stored in the inductor, the utilization factor, amplitude of a magnetic flux density in the core, and the amplitude in the current density of the winding conductor, respectively.

We designed a magnetic ferrite C-core based on the following parameters as shown in Fig.9: $K_v = 19.2$ (the rated $A : B$ and $C : D$ is set to 1:3), $K_u = 0.5$ $B_m = 0.8$ T and $J_w = 4$ A/mm^2.

Figure 10 shows the relationship between the inductor volume and the area products. From (18), (19), the volume of an inductor is proportional to the three-quarters power of the stored energy in the inductor. In this specification, the volume of the boost inductor in the active buffer can be decreased by 70% lower than the standard boost chopper.

B. Heat sink

Heat sinks are designed by concerning about the power density. At first, we calculate the cooling system performance index (CSPI) [8],[9] as

$$CSPI = \frac{1}{R_{th} V_F} \ . \tag{20}$$

Figure 11 shows a simplified thermal model. Parameters of resistance R_{th_j-c} and R_{th_c-f} are obtained from the data sheet. R_{thf} is calculated from (20) with loss analysis data.

In this paper, the heat sink is designed to meet the following specifications: CSPI = 5, Junction temperature = 125 °C, ambient temperature = 40 °C.

C. Capacitor

The design of the capacitor volume is difficult to indicate by mathematical expression. Therefore, the capacitor volume is designed based on the available market products.

Figure 12 presents three different types of capacitor that can be utilized as a DC capacitor. As can be seen in Fig. 12(a), the volume of these capacitors is proportional to the capacitance. The smallest capacitor for the proposed converter is shown in Fig. 12(a). Notice that the selection of the electrolytic capacitor must consider upon its rated ripple current. Therefore, the large capacitor of conventional converter must select in fig 12(b), and Fig. 12(c).

Figure 13 show the total volume of the passives components implemented in the conventional converters and the proposed converter. The total volume of the proposed converter is shown to decrease by 0.6 times in compared with the conventional converter. In particular, the volume of the active buffer, which includes of the boost inductor and the DC capacitor, can be reduced by approximately 60% than that of the standard boost chopper.

Table 3 shows the comparison among these converters. The efficiency of the proposed circuit is higher than the conventional circuits even the amounts of switches are increased in the proposed circuit. In addition, volume of the proposed converter is smaller than conventional circuits due to the decrement on the inductor size.

VI. CONCLUSION

This paper compares the efficiency and the volume between several single-to-three-phase PFC converters. The efficiency of the proposed converter is highest efficiency and smallest volume of these converters. In particular, the proposed converter is 1.5% higher than the conventional converter with DCM. In addition, the total volume of the proposed converter is reduced by 0.7 times than that of the conventional converter with CCM. Therefore, the converter can achieve downsizing and high-efficiency by using the proposed active buffer.

ACKNOWLEDGMENT

Fig.13 Total volume of passive components

Table 3 Comparison of the conventional CCM, DCM and proposed converter.

	Proposed converter	Conventional converter	
		CCM	DCM
Volume of converter size [cm³]	435 cm³	654 cm³	547 cm³
Volume of inductor size [cm³]	53.6 cm³	196 cm³	89cm³
Converter efficiency [%]	94.6 %	94.1%	93.1%
The number of power devices	IGBT : 8 Diode : 5	IGBT : 7 Diode : 5	IGBT : 7 Diode : 5
The number of necessary sensor	2	3	2

※This result calculated by Table 1 and 2 specifications.

[3]   Sangsun Kim; Enjeti, P.N.; "Control of multiple single-phase PFC modules with a single low-cost DSP" in *Industry Applications, IEEE Transactions*, Vol. 39, Issue: 5, 2003 , Page(s): 1379 – 1385.

[4]   Shimizu, T. Wada, K. Nakamura, N. " Flyback-Type Single-Phase Utility Interactive Inverter With Power Pulsation Decoupling on the DC Input for an AC Photovoltaic Module System " Power Electronics, IEEE Transactions on Issue Date: Sept. 2006 Volume: 21 Issue: 5, pp. 1264 - 1272, (2006)

[5]   Kuo-Hen Chao; Po-Tai Cheng; Shimizu, T. "New control methods for single phase PWM regenerative rectifier with power decoupling function" Power Electronics and Drive Systems, 2009. PEDS 2009. International Conference on, pp. 1091 - 1096.

[6]   Y. Ohnuma, J. Itoh; "A control method for a single-to-three-phase power converter with an active buffer and a charge circuit" Energy Conversion Congress and Exposition (ECCE), 2010 IEEE, pp. 1801 - 1807.

[7]   C. W.T McLyman, "Magnetic Core Selection for Transformer and Inductors, 2nd Ed., New York, NY: Marcel Dekker, 1997.

[8]   Kazimierczuk, M.K.; Sekiya, H.; "Design of AC resonant inductors using area product method" Energy Conversion Congress and Exposition, 2009. ECCE 2009. IEEE pp. 994 - 1001.

[9]   U. Drofenk, G. Laimer, and J. W. Kolar, "Theroretical Converter Power Density Limits for Forced Convection Cooling" in *PCIM Europe* 2005 pp. 608-619.

[10] Kolar, J.W.; Drofenik, U.; Biela, J.; Heldwein, M.L.; Ertl, H.; Friedli, T.; Round, S.D.; "PWM Converter Power Density Barriers" in *Power Conversion Conference - Nagoya, 2007. PCC '07*, pp. 9 - 29.

REFERENCES

[1]   Zhonghui Bing; Min Chen; Miller, S.K.T.; Nishida, Y.; Jian Sun; "Recent Developments in Single-Phase Power Factor Correction" in *Power Conversion Conference - Nagoya, 2007. PCC '07*, pp. 1520 - 1526.

[2]   Crebier, J.-C.; Revol, B.; Ferrieux, J.P.; "Boost-chopper-derived PFC rectifiers: interest and reality" in *Industrial Electronics, IEEE Transactio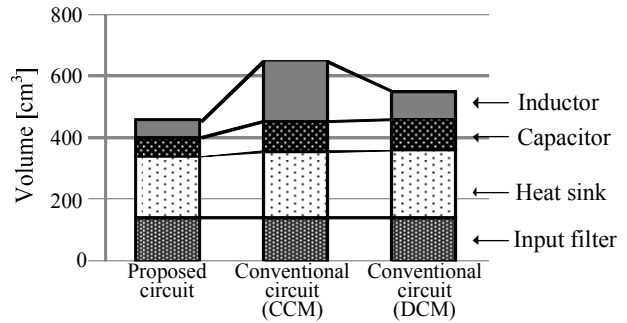ns,* Vol. 52, Issue: 1, 2005 , Page(s): 36 – 45.